BABAR-CONF-06/211
SLAC-PUB-12244
December 2006

arXiv:hep-ex/0612002v1 1 Dec 2006

Measurement of the Absolute Branching Fraction of $D^0 \to K^-\pi^+$

Romulus Godang[1] (on behalf of the *BABAR* Collaboration)
Department of Physics and Astronomy
University of Mississippi-Oxford, University, MS 38677
and
Stanford Linear Accelerator Center, Stanford University, Stanford, CA 94309.

We measure the absolute branching fraction for $D^0 \to K^-\pi^+$ using partial reconstruction of $\overline{B}^0 \to D^{*+}X\ell^-\bar{\nu}_\ell$ decays. Only the charged lepton and the soft pion from the decay $D^{*+} \to D^0\pi^+$ are used. Based on a data sample of 230 million $B\overline{B}$ pairs collected at the $\Upsilon(4S)$ resonance with the *BABAR* detector at the PEP-II asymmetric-energy B Factory at SLAC, we obtain $\mathcal{B}(D^0 \to K^-\pi^+) = (4.025 \pm 0.038 \pm 0.098)\%$, where the first error is statistical and the second error is systematic.

Presented at Joint Meeting of Pacific Region Particle Physics Communities
DPF 2006 + JPS 2006, Honolulu, Hawaii, October 29 - November 03, 2006.

Stanford Linear Accelerator Center, Stanford University, Stanford, CA 94309

Work supported in part by the U.S. Department of Energy contracts
DE-AC02-76SF00515 and DE-FG05-91ER40622.

[1]E-mail: godang@slac.stanford.edu

1 Introduction

The decay $D^0 \to K^-\pi^+$ is used as a normalizing mode in many measurements of D and B-mesons decay branching fractions. A precise measurement of the value of $\mathcal{B}(D^0 \to K^-\pi^+)$ improves our knowledge of D and B-meson properties, and of fundamental parameters of the Standard Model, such as the Cabibbo-Kobayashi-Maskawa matrix element $|V_{cb}|$ [1],[2]. The CLEO-c Collaboration has recently published a result achieving a few percent accuracy [3]. We present here a measurement of comparable precision based on partial reconstruction of the decay $\overline{B}^0 \to D^{*+}X\ell^-\bar{\nu}_\ell$, inspired by a similar measurement performed by CLEO [4]. This partial reconstruction method was introduced by ARGUS [5] to measure $B^0\overline{B}^0$ mixing, and has been exploited by DELPHI [6], OPAL [7], and CLEO [8] to measure several B-meson properties. *BABAR* applied this technique to measure the $\overline{B}^0$ meson lifetime [9], the branching fraction of $\Upsilon(4S) \to B^0\overline{B}^0$ [10], and for an improved determination of the $\overline{B}^0$ lifetime and $B^0\overline{B}^0$ oscillation frequency [11].

2 Dataset and Selection

The data sample used in this analysis consists of 210 fb^{-1}, corresponding to 230 million $B\overline{B}$ pairs, collected at the $\Upsilon(4S)$ resonance (on-resonance) and 22 fb^{-1} collected 40 MeV below the resonance (off-resonance) by the *BABAR* detector. The off-resonance events are used to subtract the non-$B\overline{B}$ background (continuum) from light quark and lepton production. A simulated sample of $B\overline{B}$ events with integrated luminosity equivalent to approximately five times the data is used for efficiency computation and background studies.

A detailed description of the *BABAR* detector and the algorithms used for particles reconstruction and identification is provided elsewhere [12]. We summarize here only the performances more relevant to this measurement. High-momentum particles are reconstructed by matching hits in the silicon vertex tracker (SVT) with track elements in the drift chamber (DCH). Lower momentum tracks, which do not leave signals on many wires in the DCH due to the bending induced by a magnetic field, are reconstructed in the SVT. Charged hadron identification is performed combining the measurements of the energy deposition in the SVT and in the DCH with the information from the Cherenkov detector (DIRC). Electrons are identified by the ratio of the track momentum to the associated energy deposited in the calorimeter (EMC), the transverse profile of the shower, the energy loss in the DCH, and the Cherenkov angle in the DIRC. Muons are identified in the instrumented flux return (IFR), composed of resistive plate chambers and layers of iron. Muon candidates are required to have a path length and hit distribution in the IFR and energy deposition in the EMC consistent with that expected for a minimum-ionizing particle.

3 Analysis Technique

We preselect a sample of hadronic events with at least four charged tracks. To reduce continuum background, we require that the ratio of the 2^{nd} to the 0^{th} order Fox-Wolfram [13] variable be $R_2 < 0.6$. We then select the sample of partially reconstructed B mesons in the channel $\overline{B}^0 \to D^{*+}X\ell^-\bar{\nu}_\ell$, searching for the charged lepton ($\ell = e,\ \mu$) and the low momentum pion (soft pion), π_s^+, daughter from the decay $D^{*+} \to D^0\pi_s^+$ [2]. This sample of events is referred to as "inclusive sample". Using the conservation of momentum and energy, in the presence of an undetected neutrino, the

[2] The inclusion of charge-conjugate reactions is implied throughout this paper.

neutrino invariant mass squared is calculated as

$$\mathcal{M}^2 \equiv (E_{\rm beam} - E_{D^*} - E_\ell)^2 - (\mathbf{p}_{D^*} + \mathbf{p}_\ell)^2 \,, \tag{1}$$

where $E_{\rm beam}$ is half the center-of-mass energy and E_ℓ (E_{D^*}) and $\mathbf{p}_\ell$ ($\mathbf{p}_{D^*}$) are respectively the center-of-mass energy and momentum of the lepton (the D^* meson). Since the B momentum ($\mathbf{p}_B$) is sufficiently small compared to $|\mathbf{p}_\ell|$ and $|\mathbf{p}_{D^*}|$, we set $\mathbf{p}_B = 0$. As a consequence of the limited phase space available in the D^{*+} decay, the soft pion is emitted nearly at rest in the D^{*+} rest frame. The D^{*+} four-momentum can therefore be computed by approximating its direction as that of the soft pion, and parameterizing its momentum as a linear function of the soft-pion momentum. The lepton momentum must be in the range $1.4 < p_{\ell^-} < 2.3\,{\rm GeV}/c$ and the soft pion candidate must satisfy $60 < p_{\pi_s^+} < 190\,{\rm MeV}/c$ in the e^+e^- center-of-mass frame. The two tracks must be consistent with originating from a common vertex, constrained to the beam-spot in the plane transverse to the beam axis. Finally, we combine p_{ℓ^-}, $p_{\pi_s^+}$ and the probability from the vertex fit in a likelihood ratio variable (χ), optimized to reject $B\overline{B}$ background. If we find more than one candidate in the event, we choose the one with the largest value of χ. We select pairs of tracks with opposite electric charge for our signal ($\ell^\mp\ \pi_s^\pm$) and use equal charge pairs ($\ell^\pm\ \pi_s^\pm$) for background studies.

We consider as signal all events where $D^{*+}\ell^-$ correlated production results in a peak near zero in $\mathcal{M}^2$. Several processes contribute to the signal: (a) $\overline{B}^0 \to D^{*+}\ell^-\bar{\nu}_\ell$ decays (primary), (b) $\overline{B} \to D^{*+}n(\pi)\ell^-\bar{\nu}_\ell$ where the $D^{*+}n(\pi)$ may or may not originate from an excited charm state (D^{**}), (c) $\overline{B}^0 \to D^{*+}\overline{D}(\tau^-)$, $\overline{D}(\tau^-) \to \ell^- X$ (cascade), and (d) $\overline{B}^0 \to D^{*+}h^-$ (fake), where the hadron ($h = \pi, K$) is erroneously identified as a lepton (in most of the cases, a muon). We also include radiative events, where one or more hard photons are emitted by any charged particle, as described by the PHOTOS package [14] in our simulation. We define a signal region as $\mathcal{M}^2 > -2$ GeV$^2/c^4$. We use the sideband region, $-10 < \mathcal{M}^2 < -4$ GeV$^2/c^4$, for background studies.

The background in the inclusive sample consists of continuum and combinatorial $B\overline{B}$ events (these last include also events where true D^{*+} and ℓ^- from the two different B mesons are combined). We determine the number of signal events in our sample by fitting the $\mathcal{M}^2$ distribution in the interval $-10 < \mathcal{M}^2 < 2.5$ GeV^2/c^4. We perform the fit in ten bins of the lepton momentum in order to reduce the sensitivity of the result to the details of the simulation. We fix the continuum contribution to rescaled off-peak events, while we scale independently the number of signal events from primary, from D^{**} and from combinatorial $B\overline{B}$ predicted by the simulation. We fix the contributions from cascade and fake decays, which account for about 3% of the signal sample, to the Monte Carlo prediction. Figure 1 shows the result of the fit in the $\mathcal{M}^2$ projection. We then determine the number of signal events with $\mathcal{M}^2 > -2$ GeV^2/c^4, as $N^{incl} = (2157.5 \pm 3.2(stat) \pm 18.1(syst)) \times 10^3$ events. The statistical error includes the statistical uncertainties of the off-peak and of the simulated events. The systematic error is discussed below.

We then look for $D^0 \to K^-\pi^+$ decays in the inclusive sample. We consider all charged tracks in the event, different from the ℓ^- and π_s^+, matching the following criteria. We combine pairs of tracks with opposite electric charge, and we compute the invariant mass $M_{K\pi}$, assigning the kaon mass to the track with charge opposite to the π_s^+ charge. No identification requirement is applied to the π^+, while the K^- satisfies its identification criterion. We select events in the wide mass range $1.82 < M_{K\pi} < 1.91$ GeV/c^2, which contains more than 95% of our signal candidates. We then combine each D^0 candidate with the π_s^+ and look for signal events in the interval $142.4 < \Delta_M < 149.9$ MeV/c^2. We use the sideband region defined by $153.5 < \Delta_M < 162.5$ MeV/c^2 for background study.

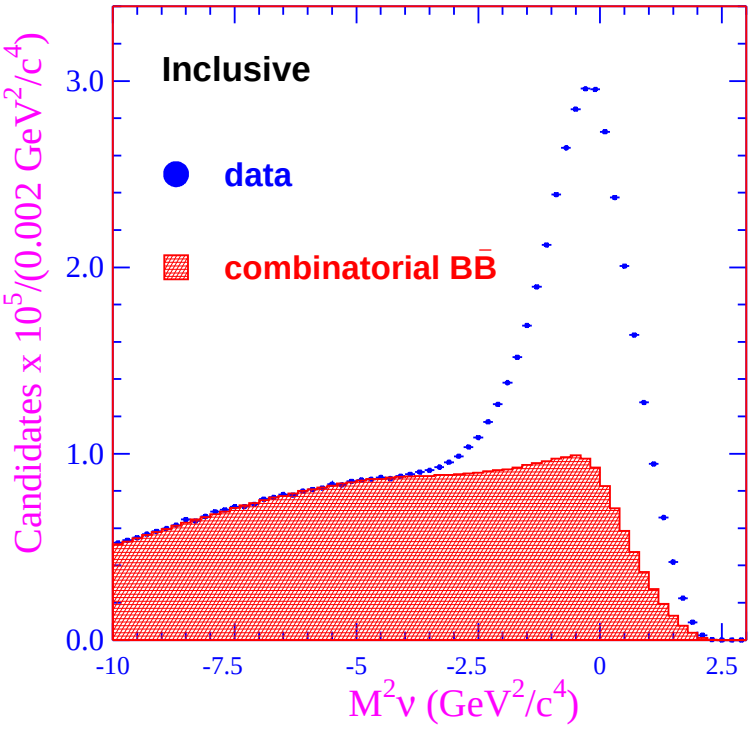

Figure 1: The $\mathcal{M}_\nu^2$ distribution of the inclusive sample. The continuum background has been subtracted. The combinatorial background has been normalized to the data.

The exclusive sample consists of signal events, and of the following background sources: continuum, combinatorial $B\overline{B}$, uncorrelated D^{*+} and Cabibbo-suppressed decays (uncorrelated peaking). We subtract the continuum using rescaled off-peak events selected with the same criteria as the on-peak data as shown in Fig. 2. Combinatorial events are due to any combination of three tracks, in which at least one does not come from the D^{*+}. We determine their number from the $B\overline{B}$ Monte Carlo. We normalize the simulated events to the data in the Δ_M sideband, properly accounting for the small fraction of signal events (less than 1%) contained in the sideband. We verify that the background shape is properly described in the simulation using a sample of D^{*+} depleted events, obtained as follows. First, we consider events in the $\mathcal{M}^2$ sideband. Then we consider "wrong flavor" events, where the candidate K^- charge is equal to the π_s^+ charge. This sample contains more than 95% combinatorial events in the signal region with a residual peaking component from Cabibbo suppressed decays (K^+K^- and $\pi^+\ \pi^-$, see below). After normalizing simulated events in the sideband, the number of events in the signal region is consistent with the data within the statistical precision of $\pm 1.3\%$.

Background from uncorrelated D^{*+} decays occurs when the D^{*+} and the ℓ^- originate from the two different B mesons. These events exhibit a peak in Δ_M but behave as combinatorial background for $\mathcal{M}^2$. We compute their number in the $\mathcal{M}^2$ sideband data, and rescale to the $\mathcal{M}^2$ signal region using the simulation events.

Cabibbo suppressed decays $D^0 \to K^-K^+$ ($D^0 \to \pi^-\pi^+$) contribute to the peaking background, where one of the kaons (pions) is wrongly treated as a pion (kaon). Simulation shows that these events peak in Δ_M, while they exhibit a broad $M_{K\pi}$ distribution. Their amount is sizeably reduced by a tighter requirement on $M_{K\pi}$. We subtract this background source using the simulation. It should be noted that the contribution from Doubly Cabibbo Suppressed decays is negligible.

We finally obtain a sample of $N^{excl} = 31700 \pm 280$, where the error is statistical only. The detailed composition of the inclusive and exclusive data sets is presented in Table 1.

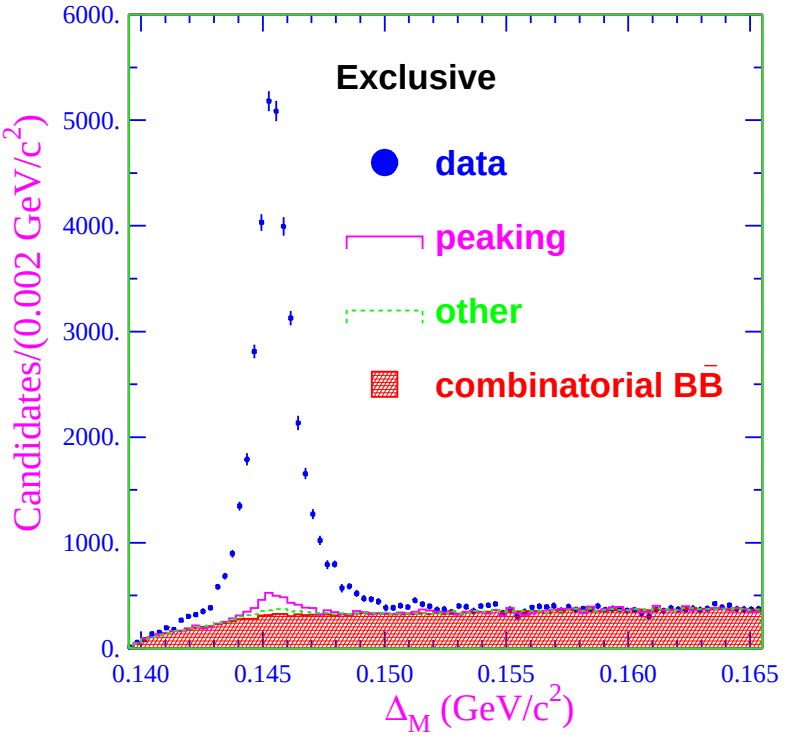

Figure 2: The Δ_M mass distribution of the exclusive sample, after continuum subtraction. The data are represented by points with its error. The hatched histogram shows the combinatorial $B\overline{B}$ background. The other histograms show the uncorrelated peaking (solid histogram) and Cabibbo suppressed decays or other (dotted histogram), respectively.

4 Branching Fraction

We compute the branching fraction as

$$\mathcal{B}(D^0 \to K^-\pi^+) \;=\; \frac{N^{excl}}{N^{incl}} \times \frac{1}{\varepsilon_{(K^-\pi^+)}\beta}, \tag{2}$$

Table 1: Composition of the inclusive and exclusive samples.

Source	Inclusive	Exclusive
Data	3887550 ± 1970	43920 ± 210
Continuum	408960 ± 1970	2940 ± 170
Combinatorial $B\overline{B}$	1321250 ± 580	7410 ± 50
Peaking	.....	1370 ± 80
Other	.....	510 ± 10
Yield	2157530 ± 2850	31700 ± 280

where $\varepsilon_{(K^-\pi^+)} = (34.78 \pm 0.10)\%$ is the D^0 reconstruction efficiency, and $\beta = 1.0496 \pm 0.0016$ is the analysis bias introduced by the partial reconstruction (see below).

The dominant contribution to the systematic uncertainty comes from the analysis bias. The bias factor β is introduced to account for the fact that the efficiency of the inclusive event reconstruction is larger for two prong D^0 final states than for other events. Examining simulation, we find three independent bias sources. First, the reconstruction of the soft-pion track is less efficient for events with a high charged-tracks multiplicity, due to the larger density of hits near the π_s^+ track. This accounts for a $(2.5 \pm 1.2)\%$ bias. A second contribution $(2.4 \pm 1.2\%)$ is due to the cases in which one of the charged tracks from the D^0 decay is preferred to the π_s^+ in forming the inclusive candidate, and then the correct combination is lost. This is more frequent for large multiplicity D^0 decays, because there are more charged tracks, and these have on average smaller momentum. Finally, the requirement on the minimal charged track multiplicity reduces by $\sim 10\%$ the number of 0-prongs D^0 decays as compared to two or more prongs. The contribution from this last effect is, however, less significant $(0.5 \pm 0.2\%)$. We take half of the deviation from unity as the systematic uncertainty on each source of the analysis bias. We consider all effects are independent and add these effects in quadrature to get a systematic uncertainty of 1.70%.

The main systematic uncertainty on N^{incl} is due to the knowledge of the combinatorial $B\overline{B}$ background (non-peaking combinatorial background). We perform a fit on the $\ell^{\pm}\pi_s^{\pm}$ background control sample as we do on signal events. We take the RMS spread of the ratio between the data and the fit in the $\mathcal{M}^2$ projection resulting in a 0.75% systematic uncertainty due to the combinatorial background (this choice is slightly more conservative than that adopted in [4]). As first noticed in [4], the decays $\overline{B}^0 \to \ell^- \bar{\nu}_\ell D^+$, with $D^+ \to K^* \rho(\omega) \pi^+$, constitute a good-charged peaking background, because the charged pion is produced almost at rest in the D^+ decays. In order to estimate the systematic uncertainty due this background, we vary its total fraction by $\pm 100\%$ in the $B\overline{B}$ events in the Monte Carlo. Then we consider all the sources of systematic uncertainty which affect the shape of the signal $\mathcal{M}^2$ shape. We vary by $\pm 30\%$ in turn the amount of events where at least one hard photon is radiated by either the ℓ or the π_s^+, or where the π_s^+ decays to a muon. We vary also by $\pm 30\%$ the fraction of cascade and fake decays, which are not determined by the fit. Finally, we vary in turn by $\pm 100\%$ the amount of events from each of the five sources constituting the D^{**} samples (two narrow and two broad resonant states, and non resonant D^{*+} pions). In each of the above studies, we repeat the fit, and take the variation in the result as the corresponding systematic uncertainty.

To estimate the systematic uncertainty due to the background subtraction on N^{excl}, we first vary the number of events from combinatorial background below the signal peak by the statistical

uncertainty as described above. We then vary by ±50% the number of signal events contained in the sideband used for background normalization, and we repeat the measurement. We vary the fraction of events from Cabibbo suppressed decays by the uncertainty on the corresponding branching fraction, as reported in [15]. As we determine the number of uncorrelated peaking events from data, the corresponding systematic uncertainty is negligible.

Uncertainties of charged-track reconstruction, kaon identification, computation of $M(D^0)$ and of Δ_M affect the determination of the efficiency. The single charged-track reconstruction efficiency is determined with ±0.5% precision. We then add linearly the error for the two tracks. The efficiency for K^- identification is measured with ±0.7% systematic uncertainty from a large sample of $D^{*+} \to D^0\pi^+, D^0 \to K^-\pi^+$ decays. When comparing a high purity signal sample, we observe a slight discrepancy between the shape of $M(D^0)$ in the data and in the simulation. We compute a systematic error of ±0.8% due to the tuning of the simulated Monte Carlo events.

We compute the final relative systematic error of 2.43% from the quadratic sum of all uncertainties listed above as shown in Table 2. We cross check this result using four other alternative

Table 2: Summary of the relative systematic uncertainties of $\mathcal{B}(D^0 \to K^-\pi^+)$.

Sample	Source	$\delta(\mathcal{B})/\mathcal{B}$ (%)
N^{incl}	Analysis bias	1.70
	Non-peaking combinatorial background	0.75
	Peaking combinatorial background	0.34
	Soft pion decays in flight	0.10
	Fake leptons	0.08
	Cascade decays	0.08
	Monte Carlo events shape	0.08
	Continuum background	0.05
	D^{**} production	0.02
	Photon radiation	0.02
N^{excl}	Tracking efficiency	1.0
	D^0 invariant mass	0.8
	K^- identification	0.7
	Combinatorial background shape	0.3
	Combinatorial background normalization	0.27
	Other background	0.1
Total		2.43

selections of the exclusive samples: (1) we do not require that the K^- to be identified, (2) we select D^0 events in a narrower (±25 MeV) band around the D^0 mass peak position, (3) we select D^0 events in a narrower band and require that the K^- and the π^+ tracks originate from a common vertex, (4) combination of selections (2), (3) above, and require that the K^- to be identified. The background varies by a factor of 10, and the efficiency by about 30%, from the looser to the tighter selection. All the results are consistent within the uncorrelated statistical and systematic uncertainties.

5 Summary

In summary, we have measured the absolute branching fraction of $D^0 \to K^-\pi^+$ with partial reconstruction of $\overline{B}^0 \to D^{*+}X\ell^-\bar{\nu}_\ell$. The preliminary result is

$$\mathcal{B}(D^0 \to K^-\pi^+) \;=\; (4.025 \pm 0.038 \pm 0.098)\%, \tag{3}$$

which is consistent with the most precise results available to-date, and has a similar precision.

6 Acknowledgments

The author would like to thank all members of the *BABAR* collaboration. This work was supported in part by the U.S. Department of Energy contracts DE-AC02-76SF00515 and DE-FG05-91ER40622.

References

[1] N. Cabibbo Phys. Rev. Lett. **10**, 531 (1963);
M. Kobayashi and T. Maskawa, Prog. Theor. Phys. **49**, 652 (1973).

[2] R. Godang (*BABAR* Collaboration), AIP Conf. Proc. **842**, 720 (2006).

[3] Q. He *et al.* (CLEO-c Collaboration), Phys. Rev. Lett. **95**, 121801 (2005).

[4] M. Artuso *et al.* (CLEO Collaboration), Phys. Rev. Lett. **80**, 3193 (1998).

[5] H. Albrecht *et al.* (ARGUS Collaboration), Phys. Lett. B **324**, 249 (1994).

[6] P. Abreu *et al.* (DELPHI Collaboration), Z. Phys. C **74**, 19 (1997).

[7] G. Abbiendi *et al.* (OPAL Collaboration), Phys. Lett. B **482**, 15 (2000).

[8] S. B. Athar *et al.* (CLEO Collaboration), Phys. Rev. D **66**, 052003 (2002).

[9] B. Aubert *et al.* (*BABAR* Collaboration), Phys. Rev. Lett. **89**, 011802 (2002).

[10] B. Aubert *et al.* (*BABAR* Collaboration), Phys. Rev. Lett. **95**, 042001 (2005);
R. Godang (*BABAR* Collaboration), Int. J. Mod. Phys. A **20**, 3605 (2005).

[11] B. Aubert *et al.* (*BABAR* Collaboration), Phys. Rev. D **73**, 012004 (2006).

[12] B. Aubert *et al.* (*BABAR* Collaboration), Nucl. Instrum. Meth. A **479**, 1 (2002);
M. S. Zisman, Ann. Rev. Nucl. Part. Sci. **47**, 315 (1997);
P. R. Burchat *et al.*, Nucl. Instrum. Meth. A **316**, 217 (1992);
P. Oddone, UCLA Workshop, eConf C870126, 423 (1987).

[13] G. C. Fox and S. Wolfram, Phys. Rev. Lett. **41**, 1581 (1978).

[14] E. Barberio and Z. Was, Comput. Phys. Commun. **79**, 291 (1994).

[15] Y.-M. Yao *et al.* (Particle Data Group), J. Phys. G **33**, 1 (2006);
E. Barberio *et al.* (Heavy Flavor Averaging Group), hep-ex/0603003 (2006).